IOP Conf. Series: Materials Science and Engineering **416** (2018) 012001 doi:10.1088/1757-899X/416/1/012001

Microstructure and Phase Composition of NiCrBSi-TiB_2 Vacuum Furnace Fused Flame-Sprayed Coatings

N Kazamer[1,2,*], P C Vălean[1,2], D T Pascal[2,*], R Muntean[2], G M Mărginean[2] and V A Șerban[1]

[1]Materials and Manufacturing Engineering Department, Politehnica University Timișoara, Piața Victoriei 2, Timișoara, 300006, Romania
[2]Materials Science and Testing Department, Westphalian University of Applied Sciences, Neidenburgerstr. 43, Gelsenkirchen, 45897, Germany

*Corresponding author: dragos.pascal@w-hs.de, norbert.kazamer@w-hs.de.

Abstract. Several studies have revealed that NiCrBSi reinforced with different intermetallic compounds exhibits characteristics that allow the material to be successfully used as a thermally sprayed coating for applications that require wear and corrosion protection. One of such materials is TiB_2, as it has an elevated melting point, high elasticity modulus, increased hardness and good thermal stability. NiCrBSi was mechanically mixed with 5%, 10%, 15% and 20% vol. TiB_2, flame sprayed and subsequently fused in a vacuum furnace. A remelting process under controlled atmosphere offer important advantages like good gas extraction and precise adjustment of temperature. The best performing batch of samples were selected for further analyse of microhardness and porosity measurements. The experimental results show that the thermal cycle created with the aid of the data offered by differential thermal analysis lead to a reduced porosity without affecting the hardness. X-ray diffractometry was used to characterize the phase composition while scanning electron microscopy was employed to investigate the microstructure and phase distribution. Further theoretical aspects regarding the influence of the phase composition on the coatings properties, like hardness or sliding wear conclude the work.

1. Introduction

Patented in 1909 by the Swiss inventor Max Ulrich Schoop [1], thermal spraying developed as a widely used technology in applications like heat exchangers, extruders, pistons, pipes or laminators [2-4]. The research in the area of Ni-based alloys began almost five decades ago [5] and shows that this type of materials can be used for a large range of technologies like flame spraying [6], Atmospheric Plasma Spray (APS) [7] or High Velocity Oxy Fuel (APS) [8].

Among the most well-known Ni-based alloys is NiCrBSi, a material used with industrial applications in respect of wear and corrosion protection [9-11]. Regarding its chemical composition, Ni as the main element influences the alloy's mechanical properties, mainly its ductility and hardness. The role of Cr is to improve the corrosion resistance while B and Si lowers the melting temperature of the material [12]. The content of B helps improving the hardness. One of the possible reinforcements for the Ni-based alloys is TiB_2, which because of its characteristics, is a suitable candidate for thermal spraying depositions. This material exhibits a high hardness, 3460 HV, low density, 4.52 g cm^{-3}, and an excellent resistance to oxidation, which goes up to 1000°C [13].

The NiCrBSi thermally sprayed products show moderate adhesion to the substrate, relatively high porosity and unwanted trapped gasses in the coatings [14]. A fusing process is therefore necessary to enhance the characteristics of the depositions and mitigate the above mentioned defects. Besides the properties previously described, B and Si also reduce the melting interval of the alloy [12], which has a positive impact for the coating post-treatment. Vacuum furnaces have recently started to be applied for such post-treatments as they offer reproducibility, the possibility of maneuvering products with complex geometries and a relative low cost with a short recoupment period [15].

The aim of the research work was to investigate the microstructure and phase composition of NiCrBSi-TiB_2 flame sprayed and vacuum fused coatings. NiCrBSi powder was mechanically mixed with TiB_2 in different volumetric concentrations, flame-sprayed and post-fused. Powder analysis, heat-treatment, microhardness measurement, porosity calculation, microstructure and phase composition examinations were all considered in the elaboration of the present work.

2. Experimental procedure

The Ni-based alloy was provided by Karl Schumacher GmbH and the NiCrBSi-TiB_2 powder was deposited on an S355JR carbon steel with 0.22% C and 1.6% Mn at the same German company. A successful deposition on a widely used steel in industry will offer the coating a larger applicability.

2.1. Feedstock powder and methods for characterisation

As one can see, Figure 1(a) shows the SEM micrograph of the NiCrBSi mixed with TiB_2. The spheroidization of Ni-based powder produced through water atomization helps the flowability through the spraying equipment. The EDX spectrum in Figure 1(b) shows the main element Ni, the hard carbide forming element Cr and Si, which promotes the wettability of the coating during deposition. The spectrum in Figure 1(c) shows Ni and the hard element Ti. The chemical composition and the size ranges of the two powders can be found in Table 1. Four sets of mechanically mixed powder with 5% (NTB5), 10% (NTB10), 15% (NTB15) and 20% (NTB20) vol. TiB_2 were prepared.

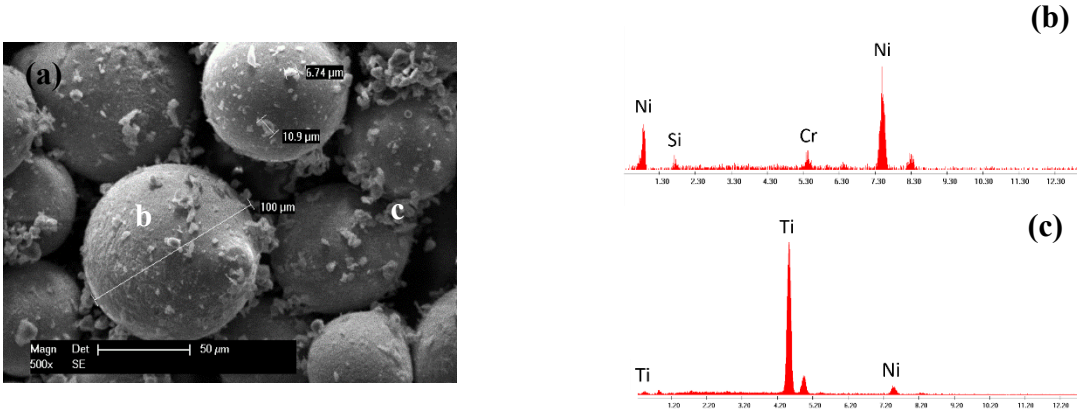

Figure 1. SE micrograph (a) of the NiCrBSi- TiB_2 mechanically mixed powder along with two EDX spectra demonstrating the chemical composition of the (b) NiCrBSi and (c) TiB_2 powder.

Table 1. Chemical composition and size range of the NiCrBSi and TiB_2 powder

	Ni [%]	Ti [%]	Cr [%]	B [%]	Si [%]	Fe [%]	C [%]	O_2 [%]	Size range [µm]
NiCrBSi	bal.		6	1	4	1.5	0.3		45-106
TiB_2		bal.		min. 30		max. 0.1	0.5	max. 1.1	6.5-10

2.2. Coating deposition and remelting

A careful thermal analysis of the powder was performed with a Netzsch STA 449F1 instrument. The DTA curve shows that all the examined powders exhibit a similar melting temperature at about 1030°C. This result has to be taken into account when selecting the fusion cycle as a temperature close to the melting point provides a densification of the coating without spilling it [16]. The surface was activated through grit blasting prior the deposition, this being a highly recommended step for a good adherence of the coating [17]. The fusion of the deposition was realised in a HITERM 80-200 vacuum furnace. Figure 3 represents the performed heating cycle which lasted a total of 288 min. with a maximum heating temperature of 1090°C with a holding time of 45 min. The ramps were set up to avoid changes during the heating and cooling steps that could have induced stress or cracks.

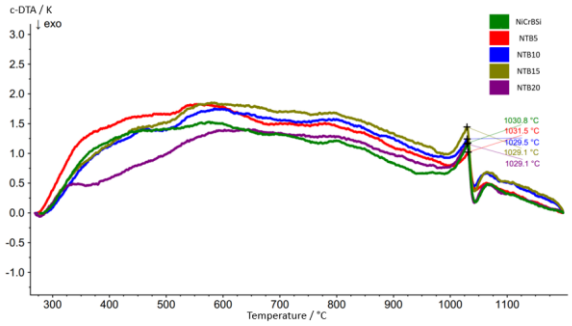

Figure 2. DTA curve highlighting the liquidus temperature of the NiCrBSi and NTB powders.

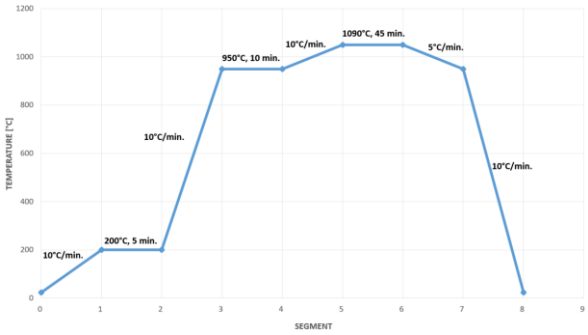

Figure 3. Vacuum furnace heating cycle of the as-sprayed samples.

2.3. Sample microhardness measurement and porosity calculation

The improvement of the post-treatment of the applied coatings was done considering the porosity and the microhardness of the samples. The porosity of the coatings was calculated on five different regions on micrographs using the image analysis software ImageJ. The microhardness tests were performed on the coating region at a load of 0.3 kgf using a Zwick/Roel ZHVμ-S machine.

2.4. Microstructure and phase composition

The quality of the coating was measured through several methods. The micrographs taken for the preliminary porosity calculation test were taken with a Leica DM-RME light microscope. The morphology, microstructure and chemical composition was studied using a Philips XL 30 SEM combined with EDX spectroscopy. The phase composition was determined using a Philips X'Pert X-ray diffractometer using a Cu K-α radiation source scattering the 2θ angle between 20° and 100°.

3. Results and discussions

3.1. Sample porosity and microhardness

The porosity level and the microhardness were chosen as the two eliminating criteria after the post-treatment of the samples. Both factors are commonly employed as excluding responses in thermal spraying [18,19] as they are directly influencing the mechanical properties of materials. Figure 4(a) represents an as-sprayed sample where a porosity level of approximately 25% in all coating batches prior the post-treatment process was measured. Figure 4(b) shows the post-fused NTB15 sample etched in a 3% HNO_3 solution. One can observe a drastic decrease of porosity, with an improved roughness, a good adhesion and no visible major defects. Porosity calculations of post-treated NTB5, NTB10, NTB15 and NTB20 can be consulted in Figure 4(c), Figure 4(d), Figure 4(e) and Figure 4(f). The NTB10 and NTB20 exhibited close mean values at 6.5±0.5% and 7.5±0.5%, respectively. The NTB5 and NTB15 performed better, showing average values of 1.5±0.5% and 0.8±0.5%, comparable

results to APS or HVOF processes. The decrease of porosity in the case of the fused samples may be attributed to the characteristics of the furnace to control and maintain the temperature, leading to the wetting of the surface offering a good gas extraction and void closure. The porosity of the coating is affected as well through the control of B and Si as they offer wettability [2] and act as fluxing agents.

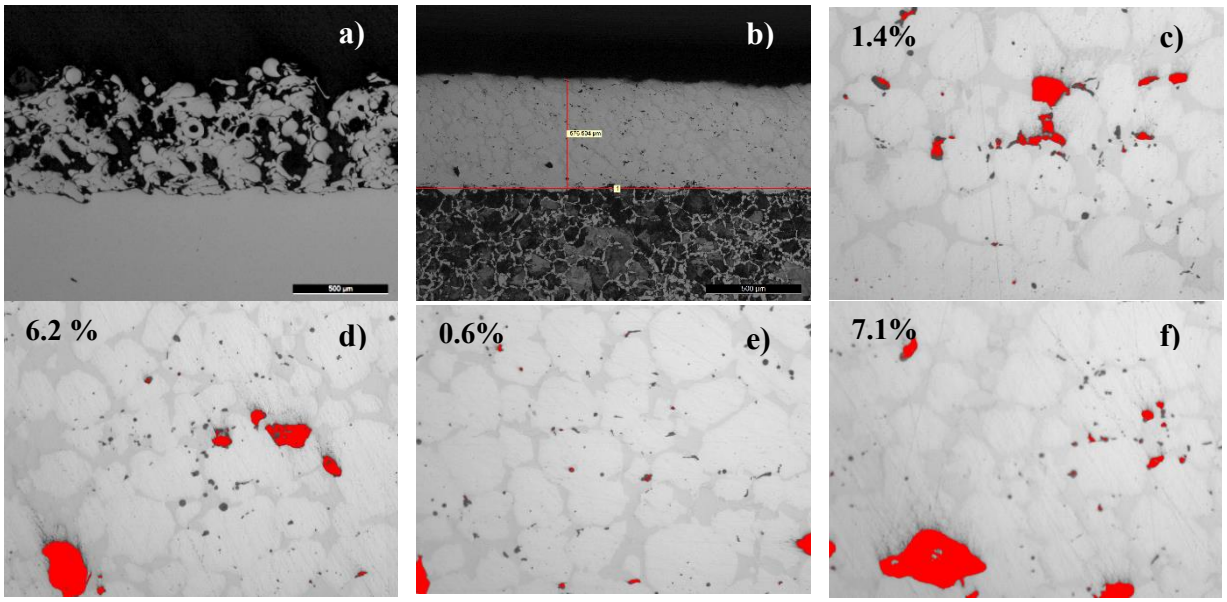

Figure 4. Light microscopy micrographs in cross-section of the a) NTB 15 as-sprayed coating, b) NTB15 post-treated coating and c) NTB5, d) NTB10, e) NTB15, f) NTB20 porosity measurements.

The microhardness of the deposited coatings was evaluated realizing seven imprints along the coating, the distribution being presented in Figure 5. The NTB10 and NTB20 coatings have both showed differences of over 30% between the extreme points of the measurement. The NTB5 coating exhibited a mean value of 225HV. The NTB15 samples showed smaller variations, the mean calculated value being 310HV. The variations of the measurements may be attributed to the different containing phases in the coating. The topography of a microindentation of the NTB15 sample presented in Figure 6 shows plastic deformation with no crack appearance, denoting a good phase bonding and low residual stresses.

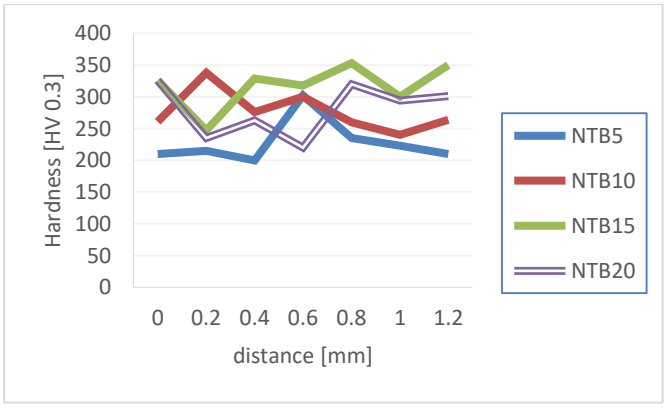

Figure 5. Graph highlighting the variation of the HV0.3 microindentation along the coating.

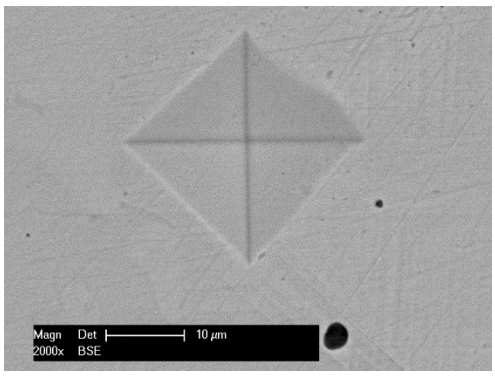

Figure 6. HV0.3 microindentation of the NTB15 sample.

Considering the porosity of under 1% and the rather constant microhardness with crack-free imprints, the NTB15 post-fused coating was chosen to be further analysed regarding its microstructure and phase composition.

3.2. Microstructure and phase composition

The NTB15 sample presented in Figure 7 exhibits a heterogeneous distribution of the dark phases TiB_2 phases. The reason for a non-homogeneous distribution lies in the mixing process of the powders and the high melting temperature of TiB_2 [13] which resists to plastic deformation and solubility in solid solutions even at high temperatures [21]. An EDX spot analysis at the interface demonstrates diffusion of Ni into the substrate creating a metallurgical bonding instead of the commonly reached mechanical hooking [22], aiding the adhesion.

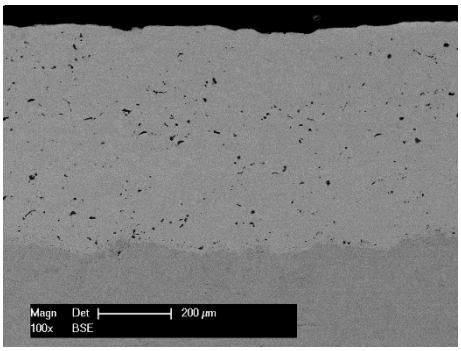

Figure 7. Cross-section SEM micrographs at lower magnification of the NTB15 sample.

Figure 8(a) shows four different regions with different chemical composition as detected by means of EDX spot analyses in Figure 8(b), Figure 8(c) and Figure 8(d). Corroborating the XRD spectra from Figure 9 with the EDX spot analyses, the matrix marked with b in Figure 8(a) mainly consists of the γ-Ni and BNi_2, similar eutectic phases being previously reported in Ni-based thermal sprayed coatings research [23-26]. Another component of the matrix is the σ-$Cr_3Ni_5Si_2$ phase, that can be found in the ternary Cr-Ni-Si diagram [27]. As previously reported by Schuster et al [28], the low Si content (4% in the present work) favours forming the σ phase.

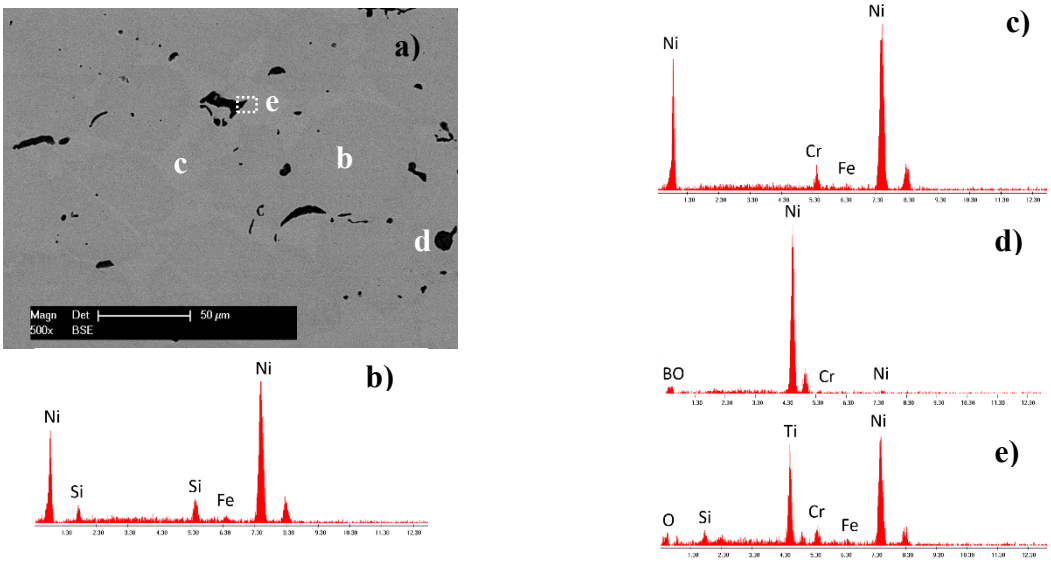

Figure 8. a) SEM micrograph of NTB15 sample along with the corresponding b), c), d), e) EDX spectra.

A confirmation that the heating cycle parameters were well chosen comes from the fact that it was not reached a temperature which transforms the Cr containing σ-$Cr_3Ni_5Si_2$ hard phase into a Ni solution along with minor constituents [29]. Observing both EDX analysis XRD results, the region c in Figure 8(a) corresponds to the rest γ-Ni/BNi_2 phase. The area d on the SEM micrograph is represented by the hard TiB_2 phase which is expected to aid the wear resistance of the coating and partly the Ti_3O. The EDX spectrum of the e area is showing a diffusion at the interface between the matrix and the TiB_2. The diffusion process forms on the one side Ti_3SiC_2, conferring high temperature stability and high fracture toughness [30], and Ti_2FeNi. The crack free microindentations may be attributed to the presence of the ductile Ti_3SiC_2 phase which is binding the matrix and the TiB_2 particles together leading to a coating with low residual stresses. The Ti_2FeNi phase with the more known empirical formula $FeNiTi_2$ may be consulted in the ternary Fe-Ni-Ti diagram [27]. The data provided by Duarte el al [31] shows that the solid solubility of Ti in (Fe,Ni) varies in dependence with the Fe:Ni ratio and lowers with decreasing temperature.

As the maximum operating pressure of the furnace vacuum pump is 10^{-6} mbar and the elimination of a large number of oxide and gases is successfully performed, Ti and Si have both according to the Ellingham diagram a high susceptibility of forming oxides until an oxygen partial pressure of about 10^{-23} mbar [32] and the formation of Ti_3O and SiO_2 is therefore inevitable. Nevertheless, in the current case the presence of Ti_3O during sliding wear tests it is proved to activate a tribofilm on the contact surfaces, resulting a decrease of the wear rate and the friction coefficient of the tribological pair [33].

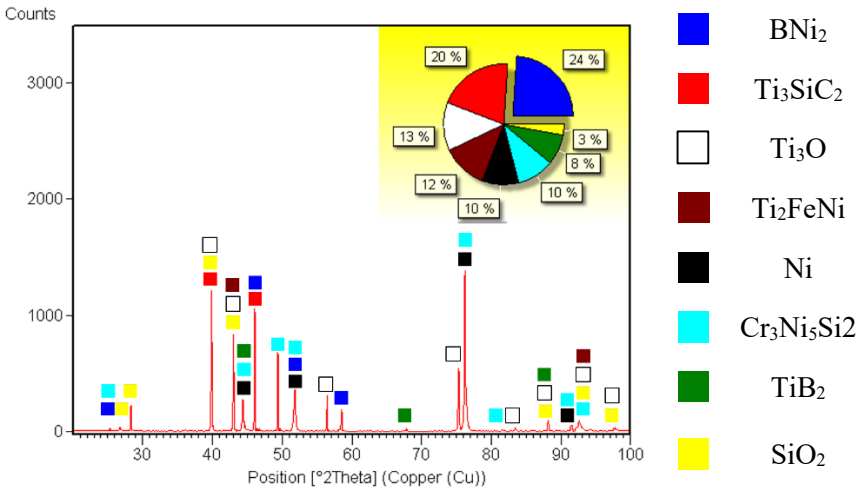

Figure 9. XRD pattern of the NTB15 sample.

4. Conclusions

Reinforcements and the improvement of self-fluxing alloys are a continuous topic in the coating industry. NiCrBSi-TiB_2 with 5%, 10%, 15% and 20% vol. concentration of TiB_2 have been successfully flame sprayed and vacuum furnace fused on a low alloyed steel. A coating with no visible major defects and a strong metallurgical bonded interface was obtained. Following the post-treatment process, considering the results of the microhardness tests and porosity measurements, the NiCrBSi-TiB_2 85-15 was further analyzed. The microstructure exhibits a heterogeneous distribution of the TiB_2 in the coating. A complex structure, with a matrix mainly composed of γ-Ni and BNi_2 was observed. The hard TiB_2 particles are partly diffused in the matrix creating Ti-based phases which offer the coating ductile properties, resisting to deformations without generating cracks. Recent research show that the presence of Ti_3O might represent a positive aspect as during sliding wear tests it activates a tribofilm decreasing the wear rate of the tribological pair. Further research could be performed in the direction of examining the deposited coating in respect for their corrosion and wear behaviour.

5. References

[1] Siegmann S and Abert C 2012 *Surface & Coating Technology* **220** 3
[2] Davis JR 2004 *Handbook of Thermal Spray Technology* vol 1, (Ohio, ASM International) p 10
[3] Lin MC, Chang LS, Lin HC, Yang CH and Lin KM 2006 *Surface & Coating Technology* **201** 3193
[4] Battez F, Viesca J and Gonzales R 2010 *Wear* **268** 325
[5] Kühn H and Morach E 1974 *Chemie Ingenieur Technik* **46** 281
[6] Chaliampalias D, Vourlias G, Pavlidou E, Skolianos S, Chrissafis K and Stergioudis G 2009 *Applied Surface Science* **255** 3605
[7] Wang Y, Stella J, Darut G, Poirier T, Liao H and Plance M-P 2017 *Journal of Alloys and Compounds* **699** 1095
[8] Kong D and Zhao B 2017 *Journal of Alloys and Compounds* **705** 700
[9] Kim HJ, Hwang SY, Lee CH and Juvanon P 2003 *Surface & Coating Technology* **172** 262
[10] Singh S and Kaur M 2016 *Surface Engineering* **32** 464
[11] Yao SH M 2014 *Materials Research Innovations* **18** S2-332
[12] Houdkova S, Vostrak M, Hruska M, Riha J, Smazalova E, Cesanek Z and Schubert J, 2013 *Proc. Int. Metal Conf. (Brno)* p 1407
[13] Wu Y, Qiu W, Yu H, Zhong X, Liu Z, Zeng D and Li S, 2011 *Applied Surface Science* **257** 10224
[14] Navas C, Colaco R, de Damborenea J and Vilar R, 2006 *Surface & Coating Technology* **200** *6854*
[15] Konakov SP and Lyapunov AI 2000 *Metal Science and Heat Treatment* **42** 84
[16] Bergant Z and Grum J 2011 *Image Analysis & Stereology* **30** 53
[17] Pawlowski L 2008 *The Science and Engineering of Thermal Spray Coatings* (Chichester: Wiley & Sons) p 53
[18] Lih WC, Yang Sh, Su CY, Huang SC, Hsu IC and Leu MS 2000 *Surface & Coating Technology* **133-134** 54
[19] Bertrand G, Bertrand P, Roy P, Rio C and Mevrel R 2007 *Surface & Coating Technology* **202** *1994*
[20] Schlichting KW, Padture NP, Jordan EH and Gell M, 2003 *Materials Science and Engineering A* **342** 120
[21] Zhu HBZ and Li ZX 2013 *Surface & Coating Technology* **235** 620
[22] Packham DE 2005 *Handbook of Adhesion,* Second Ed., (Chichester: Wiley & Sons) p 276
[23] Gonzales R, Garcia MA, Penuelas I, Cadenas M, del Rocia Fernandez Ma, Hernandez Battez A and Felgueroso 2007 *Wear* **263** 619
[24] Mrdak MR 2012 *Vojnotehnicki glasnik* **60(1)** 183
[25] Singh S and Kaur M 2016 *Surface Engineering* **32(7)** 464
[26] Karagoz M, Islak S, Buytoz S and Kurt B 2011 *Proc. 6th Int. Advanced Technol. Symposium* (Elazig, TUrkey) p13
[27] SGTE 2015 *Thermodynamic Properties of Inorganic Materials Compiled* ed A Watson and A Markus (Heidelberg: Springer) Vol. 2, Part 2 p 73 and p 194
[28] Schuster JC and Du Y 2000 *Metallurgical and Material Transactions A* **31(7)** 1795
[29] Sampath S, Neiser RA and Herman H 1993 *Journal of Materials Research* **8(1)** 78
[30] Barsoum MW, El-Raghi E, Rawn CJ, Porter WD, Wang H, Payzant EA and Hubbard CR 1999 *Journal of Physics and Chemistry of Solids* **60** 429
[31] Duarte LI, Klotz UE, Leinenbach C, Palm M, Stein F and Löffler JF 2010 *Intermetallics* **18** 374
[32] Atkins P and de Paula J 2006 Physical Chemistry : Thermodynamics and Kinetics ed Heidi Bamatter 8th Ed (New York: WH Freeman and Company) p 275
[33] Umanskyi O, Hussainova I, Storozhenko M, Terentyev O and Antononv M 2014 *Key Engineering Materials* **604** 16